Medical Engineering and Physics 69 (2019) 153–160

Contents lists available at ScienceDirect

Medical Engineering and Physics

journal homepage: www.elsevier.com/locate/medengphy

Technical note

Comparison of shoulder kinematic chain models and their influence on kinematics and kinetics in the study of manual wheelchair propulsion

Samuel Hybois[a,*], Pierre Puchaud[a,b], Maxime Bourgain[a], Antoine Lombart[a,b], Joseph Bascou[a,b], François Lavaste[a,b], Pascale Fodé[b], Hélène Pillet[a], Christophe Sauret[a]

[a] Institut de Biomécanique Humaine Georges Charpak, Arts et Métiers ParisTech, Paris, France
[b] Centre d'Études et de Recherche sur l'Appareillage des Handicapés, Institution Nationale des Invalides, Créteil, France

ARTICLE INFO

Article history:
Received 19 April 2018
Revised 3 April 2019
Accepted 6 June 2019

Keywords:
Wheelchair
Musculoskeletal modeling
Ellipsoid mobilizer
Shoulder

ABSTRACT

Several kinematic chains of the upper limbs have been designed in musculoskeletal models to investigate various upper extremity activities, including manual wheelchair propulsion. The aim of our study was to compare the effect of an ellipsoid mobilizer formulation to describe the motion of the scapulothoracic joint with respect to regression-based models on shoulder kinematics, shoulder kinetics and computational time, during manual wheelchair propulsion activities. Ten subjects, familiar with manual wheelchair propulsion, were equipped with reflective markers and performed start-up and propulsion cycles with an instrumented field wheelchair. Kinematic data obtained from the optoelectronic system and kinetic data measured by the sensors on the wheelchair were processed using the OpenSim software with three shoulder joint modeling versions (ellipsoid mobilizer, regression equations or fixed scapula) of an upper-limb musculoskeletal model. As expected, the results obtained with the three versions of the model varied, for both segment kinematics and shoulder kinetics. With respect to the model based on regression equations, the model describing the scapulothoracic joint as an ellipsoid could capture the kinematics of the upper limbs with higher fidelity. In addition, the mobilizer formulation allowed to compute consistent shoulder moments at a low computer processing cost. Further developments should be made to allow a subject-specific definition of the kinematic chain.

© 2019 IPEM. Published by Elsevier Ltd. All rights reserved.

1. Introduction

Manual wheelchairs (MWC) can help people with physical impairments to regain independent mobility. This is a primary factor for autonomy, improving social connection, active participation and self-reliance [1]. However, due to the repetitive and demanding motion of the upper limbs, MWC propulsion can induce overuse pain and injuries [2,3]. To overcome such issues, some studies have investigated the influence of MWC configuration on propulsion effort [4–10]. These studies showed that settings such as axle position, seat height and anterior-posterior position influenced upper limbs biomechanics (muscle forces and kinematics) and handrim biomechanics (push and release angles, handrim forces). Another branch of MWC propulsion optimization was investigated with the biomechanical effect of various propulsion techniques [11–15]. It showed that MWC propulsion patterns (arcing, single-loop, double-loop and semi-circular) impacted muscle forces, articular loading and energy expenditure of the upper limbs, along with spatiotemporal parameters like cadence. These studies have allowed to introduce general clinical guidelines during the prescription of a MWC [16,17]. However, some questions remain unanswered when investigating the subject-specific effects of certain MWC configurations or propulsion techniques, with the purpose of reducing both muscular and articular demands.

To achieve such a goal, a first step is to understand the mechanical behavior of the upper limbs during MWC activities. The quantification of upper limb kinematics is challenging because soft-tissue artifacts (STA) limit the accuracy of motion capture-based methods [18] and particularly for the scapula [19]. Technical marker clusters positioned on the acromion or on the spine of the scapula have been proposed to non-invasively capture the motion of this bone during dynamic activities [20–24]. Kinematics of the upper limb can then be combined with the measure of external forces applied by the user on the MWC to assess net joint moments from inverse dynamics computational methods.

* Corresponding author.
E-mail address: samuel.hybois@ensam.eu (S. Hybois).

https://doi.org/10.1016/j.medengphy.2019.06.002
1350-4533/© 2019 IPEM. Published by Elsevier Ltd. All rights reserved.

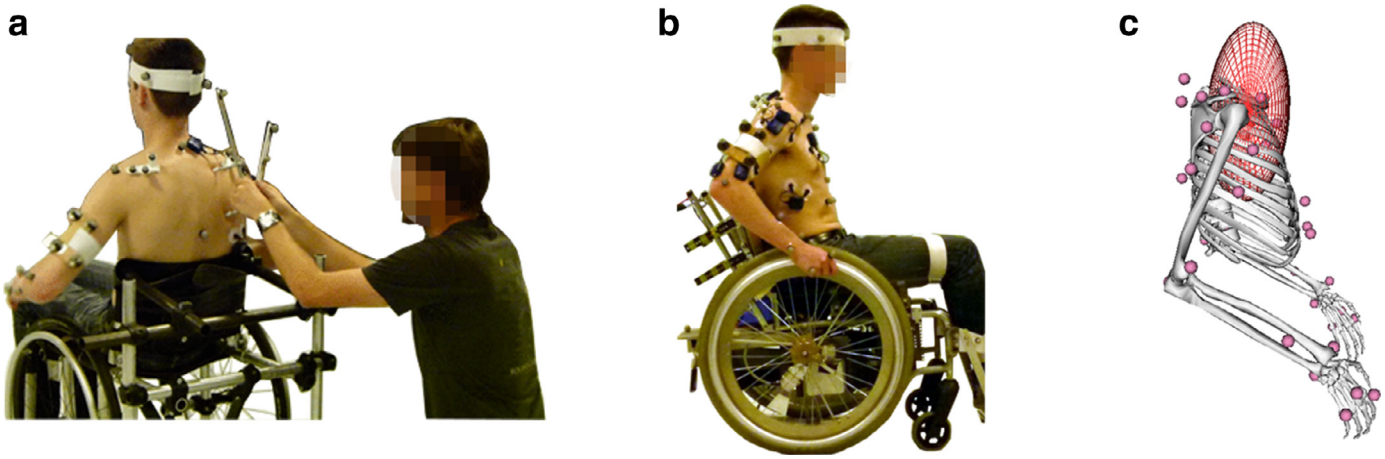

Fig. 1. (a) Calibration of the right scapular spine cluster position with a scapula locator. The left scapula spine cluster can be seen on the left shoulder of the subject. (b) Experimental protocol with the instrumented field wheelchair. (c) Musculoskeletal model developed (M_{ellips}), with the ellipsoid mobilizer in red.

To limit STA-related inaccuracies, multibody kinematic optimization (MKO), which relies on the definition of a kinematic chain, seemed to be a promising approach [25,26] and recent publications reported an accuracy improvement reaching 40–50% for scapulohumeral rotation using this technique [27,28]. However, several formulations have been developed when modeling the kinematic chain of the shoulder complex with the connection between the thorax and the scapula being an ambitious challenge. One of the first musculoskeletal models used to investigate MWC propulsion was the Delft Shoulder and Elbow model [29,30]. It described the scapulothoracic joint as a tangent gliding plane on an ellipsoid [29–32] and allocated three degrees of freedom (DoF) to the glenohumeral and acromioclavicular joints. However, this model was generally not scaled to fit the anthropometrics of each subject even if the benefit of such a procedure on the kinematic accuracy was shown a few years later [33]. Moreover, scaling the model remained difficult to perform properly. An upper extremity model available with the OpenSim software [34,35] has also been used to investigate MWC propulsion [11,36–38]. It had the benefit of being open-source, thus available to the whole research community, but was characterized by several coupling regression equations [39] to describe the 3D motion of both the clavicle and the scapula with respect to humeral elevation, namely the scapulohumeral rhythm. This model was built to allow the scaling of geometrical and inertial properties, but regression equations were believed to limit the use of this model in complex movement configurations. Previous studies already showed that the scapulothoracic joint can be modeled by a contact ellipsoid [40,41] and an ellipsoid mobilizer formulation (i.e. without kinematic constraints) was recently implemented in OpenSim [42,43]. This model was assumed to be more physiological when describing complex motions of the shoulder and was proven to be computationally efficient. However, it has only been used to investigate single-joint arm movements and not functionally relevant tasks.

The aim of this study was therefore to compare the effect of an ellipsoid mobilizer formulation, with respect to a regression-based model and a fixed-glenohumeral joint model, on shoulder kinematics (glenohumeral joint center displacement, joint angles, marker reconstruction errors), shoulder kinetics (glenohumeral net joint moments) and computer processing time, during the analysis of MWC propulsion tasks (start-ups and straight steady-state propulsion) collected from human subjects. We hypothesized that the ellipsoid mobilizer formulation would allow a better kinematic reconstruction of the wheelchair propulsion, with a subsequent impact on net joint moments at the shoulder.

2. Material and methods

2.1. Population

Following approval by the relevant ethics committee (CPP Paris VI Pitié Salpêtrière, France no. 2014-A01203-44), ten subjects with various levels of disability were involved in this study, to increase variability in upper limb kinematics and propulsion techniques. They were previously informed of the protocol and gave their written informed consent before the beginning of the experiments. The inclusion criterion imposed that subjects were experienced with MWC propulsion and did not present any shoulder pain or injury at the time and within the six months before the beginning of the experiments. The population included people with the following levels of disability and MWC expertise: 2 able-bodied who received a 3-weeks MWC practice training, 1 poliomyelitis, 1 with spinal amyotrophy, 1 with congenital malformation, 3 with paraplegia and 2 with lower limb amputation who were elite wheelchair sports athletes. The characteristics of the subjects were as follows: age: 32.9 years old (SD: 6.9 y.o.; range: 24–46 y.o); height: 1.70 m (SD: 0.09 m; range: 1.48–1.80 m); mass: 69.8 kg (SD: 7.8 kg; range: 48–80 kg).

2.2. Experiments

During the experiments, each subject was equipped with a total of 38 skin reflective markers placed on the torso, the head and on both upper limbs. The motion of the scapula was also tracked using a technical cluster composed of 3 reflective markers, placed on the spine of the scapula (as in the work by Morrow et al. [24]; see Fig. 1). Markers locations were recorded with an 8-cameras optoelectronic motion capture system (Vicon system, Oxford Metrics Inc., UK) at a rate of 100 Hz. Before the experiments, the location of the scapula spine cluster on the musculoskeletal model was calibrated with a scapula locator device during a static pose (Fig. 1(a)). Each subject then propelled a dedicated wireless field instrumented MWC over 10 m in a motion analysis laboratory covered with linoleum. Forces and torques applied by the hands on the handrims, seat, backrest and footrest were recorded at a 100 Hz frequency with a wireless field instrumented MWC (FRET-2, Fig. 1(b)) and synchronized with the motion capture system. This instrumented wheelchair (TSR-mesures, France [44–46]) was adjusted with standard settings that remained unchanged between participants (weight: 38 kg; wheelbase: 430 mm). All participants completed the entire acquisition sessions. One start-up cycle and

one steady-state propulsion cycle were processed for each subject. For start-up, subjects were asked to start from the center of the motion capture system calibrated volume and to perform 3 to 4 pushes. In this task, only the first push was analyzed. For steady-state propulsion, subjects started outside the calibrated volume, were pushed by an assistant to favor the ignition of linear velocity, and were asked to perform 6 to 7 pushes, with one cycle (the third or fourth) entirely captured within the calibrated volume of the motion capture system.

2.3. Model

A custom-made musculoskeletal model of the thorax and both upper limbs (referred to as M_{ellips}) was designed in OpenSim. The definition of the kinematic chain was based on the unilateral scapulothoracic joint model developed by Seth et al. [43]. Since this model was limited to the thorax and right-side shoulder, it was extended to a full shoulder-to-hand kinematic chain and symmetrized to result in a bilateral model (Fig. 1(c)). The resulting M_{ellips} model displayed 2 DoF at the clavicle, 4 DoF between the scapula and thorax (ellipsoid joint), 3 DoF at the glenohumeral joint and 2 DoF at both the elbow and the wrist. A geometrical contact constraint between the clavicle and scapula was added at the acromion. For comparison purposes, this M_{ellips} model was modified to result in a second model (M_{regr}) with an identical kinematic chain except for the shoulder joint description, which was chosen identical to the upper extremity model from Holzbaur et al. [34] and Saul et al. [35]. This M_{regr} model did not display independent scapula DoF with respect to the thorax, but involved several coupling regression equations. As opposed to M_{ellips}, this second model thus inferred sternoclavicular motion from scapular orientations via regression methods. Finally, a third model (M_{fix}) was derived from M_{ellips}, with the scapula and clavicle locked, resulting in the 3-DoF glenohumeral joint to represent the whole shoulder. Aside from the shoulder joint definition, all parameters (segment mass and inertia, other joint definitions) were identical for the three models. The 3 versions of the models were generic, but a homothetic scaling was applied to each bony segment independently, based on distances between markers. This scaling step of the models was performed for each subject of the population. Kinematic data (marker trajectories) and kinetic data (handrim and seat forces) collected for each subject were fed into the model, with a process detailed below.

2.4. Data processing

Markers trajectories were smoothed with an average sliding window (5 values) with 2-passes in reverse direction to minimize the shifting effect. Gaps in trajectories were filled using a C2-spline interpolation (gaps shorter than 15 frames, i.e. 0.15 s) or using a rigid registration method [47] based on the other markers of the same segment (gaps longer than 15 frames). Data processing was performed with OpenSim 3.3 [48], identically for the three models. First, model geometries and inertial parameters were scaled to the anthropometry of each subject, based on anatomical landmarks located with markers (or palpated with the scapula locator device in the case of the scapula). Afterwards, MKO [25] was performed to compute the generalized coordinates of the models using the inverse kinematics algorithm implemented in OpenSim, with both anatomical and technical markers trajectories as inputs. This was performed during steady-state propulsion and start-up cycles. Net joint moments were obtained using a Newton–Euler recursive inverse dynamics algorithm, expressed in the thorax orthonormal coordinate system, centered on the humeral head center [49,50], to favor clinical interpretation and comparison between models.

2.5. Data analysis

To compare the influence of the different shoulder models on marker reconstruction, root mean squared errors (RMSE) between experimental and reconstructed markers were computed and then averaged by segment. The evaluation of multibody kinematic optimization was made with the assumption that a lower RMSE denoted a better kinematic reconstruction. The comparison in kinematics also included the displacement of the glenohumeral joint center in the thorax reference frame (computed following ISB recommendations [51]) and joint angles which are the DoF of the model (i.e. clavicle protraction/retraction and clavicle elevation/depression). Mean values of the net shoulder moments (i.e. flexion/extension, internal/external rotation and total) along each cycle were computed and compared between models, as well as peak values over the entire cycle, that were reached during the push phase. Peak values of the flexion and internal rotation components were also reported.

The computer processing time with the different models was estimated for each subject on a conventional desktop computer (Windows 7, Intel® Xeon® CPU 2.80 GHz, RAM: 6 GB). It was defined as the time needed to execute a workflow composed of multibody kinematics optimization (3D motion capture file of a steady-state propulsion cycle as input) and inverse dynamics (generalized coordinates and external forces as inputs), using the scaled model of the corresponding subject.

2.6. Statistics

For each calculated variable, mean values and standard deviations were computed and reported over the whole population for each task (start-up and steady-state propulsion).

3. Results

3.1. Kinematics

The acromion marker translation in the thorax reference frame, averaged over the 10 subjects was greater in the anterior-posterior direction than in the vertical direction (see Table 1). Subsequently, to track this motion in the frontal and transversal planes, musculoskeletal models that enabled the mobility of the clavicle (i.e. models M_{ellips} and M_{regr}) exhibited variations of their sternoclavicular generalized coordinates (i.e. joint angles) during both steady-state propulsion and start-up (Fig. 2). The inter-individual variability of sternoclavicular angles, which can be assessed by the standard deviation corridor, was also higher with M_{ellips} than with M_{regr} (Fig. 2). Because of this movement of the clavicle, M_{ellips} displayed the highest amplitude for the glenohumeral joint center displacement in the thorax reference frame (Table 1), in both anterior-posterior and vertical directions (Fig. 3). Model M_{regr} showed only a narrow range of motion for the glenohumeral joint center, while it remained fixed for $M_{fix,}$ by definition.

Finally, the evaluation of the reconstructed kinematics, performed by computing the RMSE per segment between experimental and reconstructed markers, showed that the M_{ellips} model resulted in a limited error compared to M_{regr} and M_{fix} (Table 1) for both tasks (steady-state propulsion and start-up). Comparison between M_{regr} and M_{fix} showed that M_{regr} resulted in lower RMSE than M_{fix} for proximal segments (thorax, clavicle, and scapula) but not for distal segments (arm, forearm). The distribution of the overall reconstruction error (i.e. RMSE averaged over the whole marker set) along the cycle showed that for the M_{ellips} model, the reconstruction was slightly better during the recovery phase than during the push phase (Fig. 5). Conversely, the timing of the peak

Table 1
Summary of the biomechanical outputs of the study, averaged over the 10 subjects (standard deviations between brackets). For comparison, steady-state propulsion and start-up cycles are separated, as well as the model versions (M_{ellips}, M_{fix} and M_{regr}).

		Steady-state propulsion			Start-up		
Acromion translation [mm]	Anterior-posterior	39 (12)			44 (11)		
	Vertical	32 (10)			33 (9)		
Model version		M_{ellips}	M_{fix}	M_{regr}	M_{ellips}	M_{fix}	M_{regr}
RMSE per segment [mm]	Thorax	15 (5)	25 (5)	26 (5)	16 (5)	25 (4)	30 (4)
	Clavicle	10 (3)	13 (4)	15 (4)	11 (4)	13 (4)	18 (4)
	Scapula	18 (6)	28 (7)	28 (8)	17 (5)	25 (6)	30 (8)
	Arm	22 (10)	31 (12)	26 (10)	23 (11)	33 (15)	27 (12)
	Forearm	15 (5)	39 (11)	16 (5)	16 (5)	40 (14)	17 (5)
	Hand	10 (2)	52 (14)	12 (2)	12 (3)	53 (17)	13 (3)
Peak flexion moment [Nm]		10.3 (6.1)	5.4 (4.2)	8.2 (5.3)	23.4 (12.6)	15.3 (11.3)	20.7 (11.5)
Peak internal rotation moment [Nm]		23.3 (8.1)	24.5 (7.8)	23.9 (7.9)	28.1 (7.3)	31.1 (8.1)	29.5 (7.0)
Mean total shoulder moment [Nm]		7.8 (1.9)	8.0 (1.7)	7.9 (1.8)	15.2 (4.6)	15.5 (4.5)	15.3 (4.5)
Peak total shoulder moment [Nm]		26.2 (8.1)	26.1 (7.2)	26.0 (7.7)	37.4 (9.2)	35.6 (8.7)	36.2 (8.6)
Glenohumeral joint center	Anterior-posterior	32 (11)	0 (0)	0.13 (0.07)	34 (10)	0 (0)	0.13 (0.06)
displacement [mm]	Vertical	29 (10)	0 (0)	0.09 (0.04)	28 (10)	0 (0)	0.08 (0.04)
Computation time [s]		14.0 (1.0)	15.5 (1.1)	55.5 (12.3)			

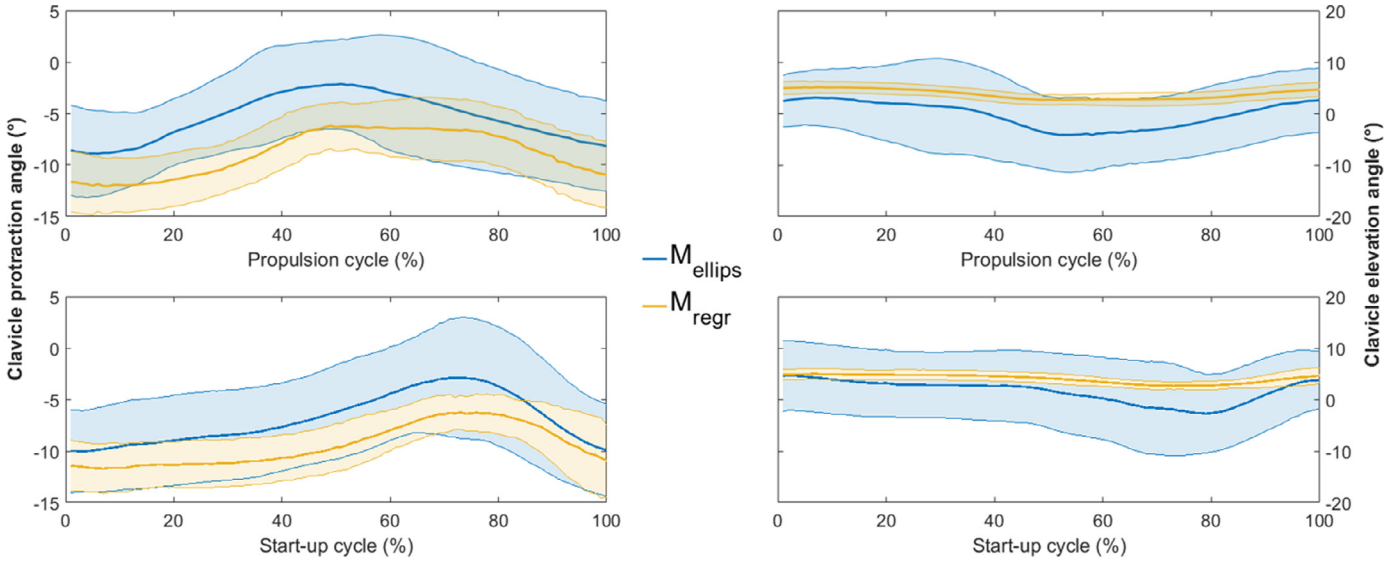

Fig. 2. Sternoclavicular generalized coordinates averaged over the 10 subjects (mean in bold line ± 1 standard deviation in shaded). Red: computed with M_{ellips} model; Blue: computed with M_{regr}; Left: clavicle protraction; Right: clavicle elevation; Top: propulsion; Bottom: start-up.

error for M_{regr} occurred at the transition between the push and recovery phases, while M_{fix} displayed its lowest reconstruction error at the end of the push phase.

3.2. Kinetics

Resulting net shoulder moments varied depending on the version of the musculoskeletal model used to perform the inverse dynamics process (Table 1, Fig. 4). Peak internal rotation and peak total shoulder moments displayed similar values between models, as well as the mean resulting shoulder moment. However, the flexion component (in the sagittal plane) varied noticeably among models.

3.3. Computer processing time

Finally, in terms of computation performance, the computer processing time was the lowest for M_{ellips} (14.0 ± 1.0 s). Similar values were obtained for M_{fix} (15.5 ± 1.1 s) but M_{regr} resulted in higher computation time (55.5 ± 12.3 s).

4. Discussion

Experimental data showed a displacement of the acromial marker with respect to the thorax, especially in the fore-aft direction. This result underlined the necessity to allow sternoclavicular mobility when analyzing MWC propulsion. The inter-individual variability of the sternoclavicular angles, which were greater with M_{ellips} than with M_{regr}, proved that model M_{regr} favored a particular motion of the clavicle due to the prediction equation based on the arm elevation. Hence, model M_{regr} hindered to reproduce the propulsion technique for individuals of the population who spontaneously engaged their clavicle in protraction/retraction. This is emphasized for this activity because MWC propulsion mainly occurs in the sagittal plane with low humerus elevation angles. Therefore, an advantage of the M_{ellips} model is its flexibility to potentially account for differences due to the level of disability, which is not possible with the other models.

The M_{ellips} model showed an improved RMSE for each segment of the upper limbs kinematic chain, with respect to other models. The reconstruction errors obtained were consistent with those reported by Blache and Begon [52], which ranged from 7 to 23 mm for analytical, sports-related and daily life movements. The ability of M_{ellips} to reproduce the motion of the upper limbs should be related to the scapula mobility on the ellipsoid, which resulted in a larger glenohumeral joint center displacement (Fig. 3). Conversely, the M_{regr} model, despite its theoretical ability to describe the glenohumeral motion, resulted in a quasi-fixed position of the

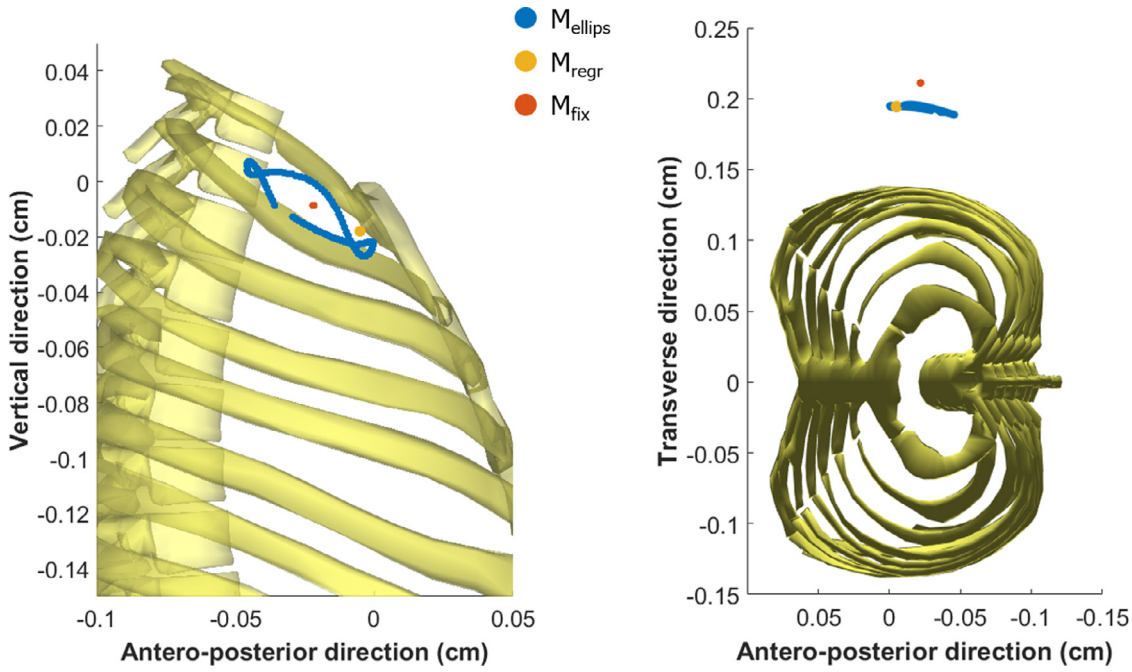

Fig. 3. Successive positions of the glenohumeral joint center computed with the three models in the thorax reference frame along a propulsion cycle for one subject.

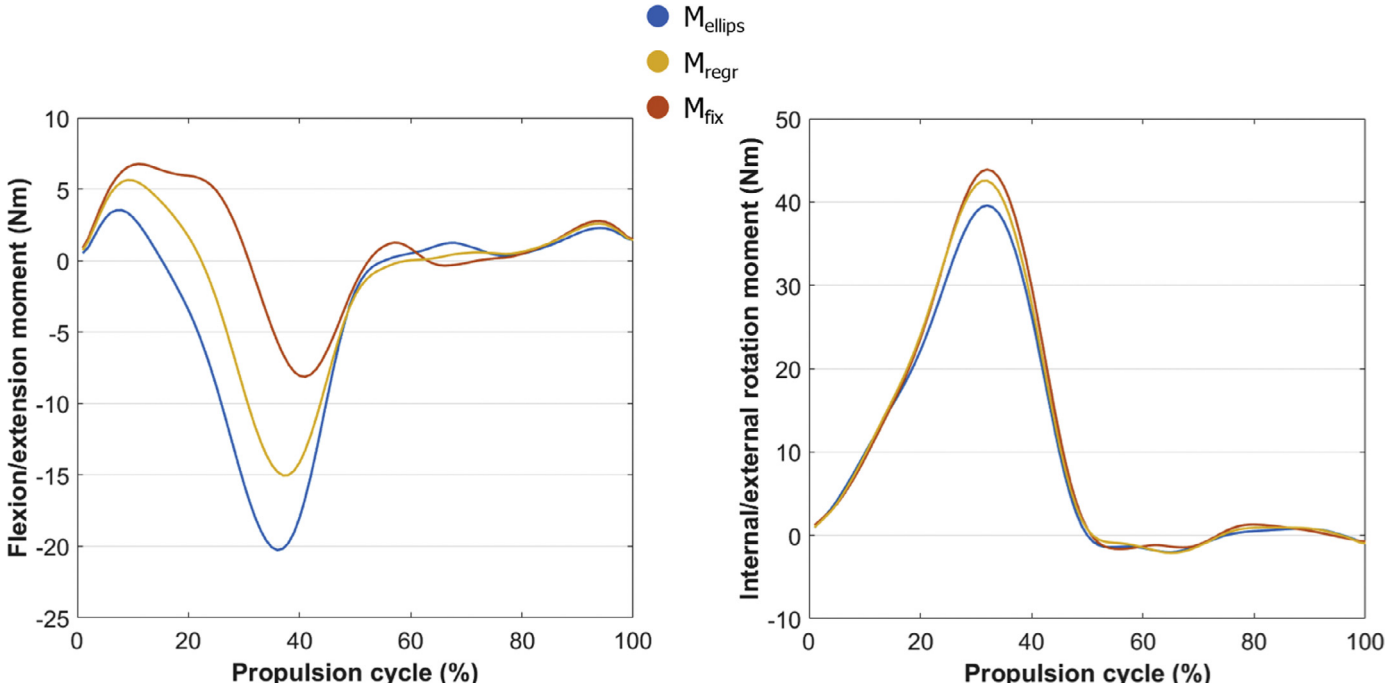

Fig. 4. Illustration of typical shoulder flexion (negative)/extension and internal (positive)/external rotation moments for one specific subject of the cohort during a steady-state propulsion cycle.

glenohumeral joint center during the cycle (Fig. 3 and Table 1) due to the low arm elevation during MWC propulsion.

In addition, the differences in the glenohumeral joint center location between models impacted the lever arms of handrim forces, which mainly explain the differences in the resulting net shoulder moments. This could lead to a change in the sign of the joint moment and consequently to differences in muscles recruitment.

The average of peak flexion moment during the push phase obtained with model M_{ellips} was consistent with values already reported in the literature [45,53]. The resulting glenohumeral joint moment displayed similar values to those reported in the study of Vegter et al. [54]. It is important to note, however, that such comparisons should be made cautiously because the coordinate systems in which moments were expressed largely varied in the literature investigating MWC shoulder kinetics [49,55–63].

As mentioned in the paper introducing the scapulothoracic joint model [43], in which the computational speeds were reportedly faster than real time, the ellipsoid mobilizer approach enabled the computer processing time to be drastically reduced with M_{ellips} compared to M_{regr}. Owing to the higher number of segments used in the present study than in the work of Seth et al. [43], however, it was not possible to achieve real-time computation with

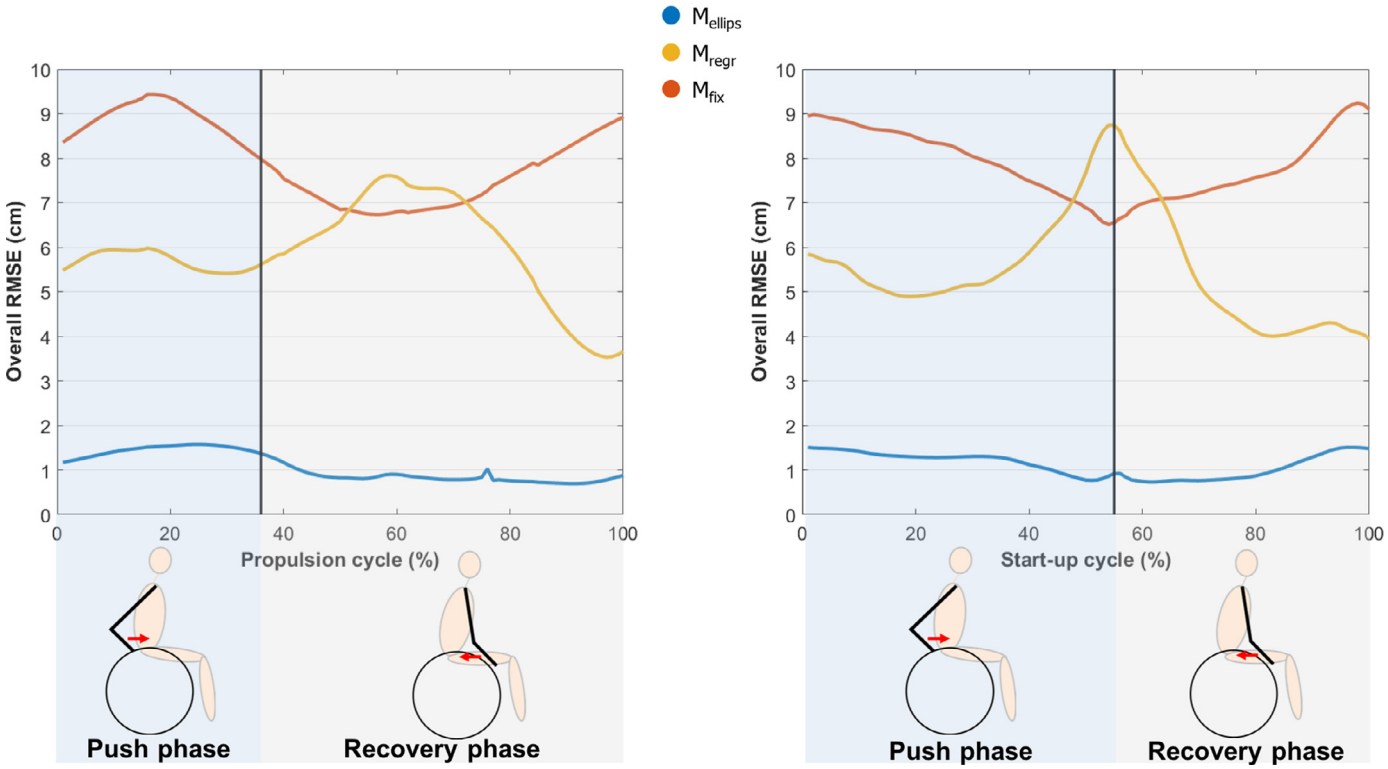

Fig. 5. Evolution of the overall marker reconstruction errors along a typical locomotion cycle (push phase + recovery phase) for one specific subject of the cohort.

a 100 Hz frame rate. Another explanation for the differences between the present study and that of Seth et al. [43] may lie in the measurement protocols, namely the use of intracortical bone pins for markers on the scapula and the subject-specificity of the ellipsoid parameters and clavicle length.

This study does have certain limitations, however. First of all, since this work aimed at embracing a modeling approach, participants were recruited from a convenience sample. This was a limit when drawing subject-specific conclusions about the effects of the model but allowed to apply the method on multiple individuals with various propulsion techniques. A subsequent limitation was that the small size of population questioned the relevance of a statistical analysis, since only one cycle was analyzed for each participant. Apart from mean and standard deviations, the authors decided not to include any statistics. However, on a set of ten subjects with different levels of disability, this study demonstrates the forces and weaknesses of three upper-limb kinematic chains when studying MWC propulsion biomechanics. Due to the multiple embedded sensors, the instrumented MWC used for the experiments was also significantly heavier than most of the conventional MWC. This may have led some participants to modify the biomechanics of their upper limbs during propulsion when compared to their own MWC. However, this should not challenge the application of results since MWC propulsion parameters (linear speed, contact and release angles, push and recovery phases temporal parameters, handrim forces and torques etc.) were in accordance with previously reported results from experiments performed with lightweight wheelchairs [45,64]. Finally, another limitation of this study is that no gold-standard is provided to directly evaluate the accuracy of joint angles with the different models. Such a comparison would have required the use of intracortical bone pins, which is a highly invasive technique whose regular use would be ethically questionable. In addition, intracortical bone pins require anesthesia that would limit the motion and their fixations can also cause discomfort or pain modifying the studied motion. However, the results of this study are not challenged by the absence of gold standard for kinematics because even if slight differences can exist between real scapula motion and scapula cluster [65], only the ellipsoid model is able to track the motion of the scapula during MWC propulsion.

5. Conclusion

This study aimed at comparing the shoulder kinematics and kinetics during MWC propulsion, computed with musculoskeletal models displaying different kinematic chains: either implemented with an ellipsoid mobilizer, regression equations, or with no scapula movement in the thorax coordinate system. The results showed the relevance of modeling the scapula as gliding on an ellipsoid [29,43], which is a more physiological description, in comparison with musculoskeletal models based on regression equations [34,35]. The model derived from the work of Seth et al. [43] displayed the best markers reconstruction, and was able to both capture subject-specific propulsion techniques and provide shoulder moments consistent with values reported with current models such as the one from Holzbaur et al. [34] and Saul et al. [35]. Another benefit of the mobilizer approach is its ability to drastically reduce the computer processing time. To pursue investigation, subject-specific methods should be developed to define the kinematic chain, especially the scapulothoracic ellipsoid parameters (center, orientation and radii) and the clavicle length. This is a crucial step before computing muscle forces and drawing clinical conclusions.

Conflicts of interest

The authors declare they have no financial or personal relationship with other people or organization that could inappropriately influence their work.

Funding

None.

Ethical approval

The study protocol was approved by the relevant ethics committee CPP Paris VI Pitié Salpêtrière, France (Ref. no. 2014-A01203-44).

References

[1] Finlayson M, van Denend T. Experiencing the loss of mobility: perspectives of older adults with MS. Disabil Rehabil 2003;25:1168–80.
[2] Boninger ML, Dicianno BE, Cooper RA, Towers JD, Koontz AM, Souza AL. Shoulder magnetic resonance imaging abnormalities, wheelchair propulsion, and gender. Arch Phys Med Rehabil 2003;84:1615–20.
[3] Curtis KA, Drysdale GA, Lanza RD, Kolber M, Vitolo RS, West R. Shoulder pain in wheelchair users with tetraplegia and paraplegia. Arch Phys Med Rehabil 1999;80:453–7.
[4] Sprigle S, Huang M. Impact of mass and weight distribution on manual wheelchair propulsion torque. Assist Technol 2015;27:226–35.
[5] Boninger ML, Baldwin M, Cooper RA, Koontz A, Chan L. Manual wheelchair pushrim biomechanics and axle position. Arch Phys Med Rehabil 2000;81:608–13.
[6] Kotajarvi BR, Sabick MB, An K-N, Zhao KD, Kaufman KR, Basford JR. The effect of seat position on wheelchair propulsion biomechanics. J Rehabil Res Dev 2004;41:403–14.
[7] Samuelsson KAM, Tropp H, Nylander E, Gerdle B. The effect of rear-wheel position on seating ergonomics and mobility efficiency in wheelchair users with spinal cord injuries: a pilot study. J Rehabil Res Dev 2004;41:65.
[8] Richter WM. The effect of seat position on manual wheelchair propulsion biomechanics: a quasi-static model-based approach. Med Eng Phys 2001;23:707–12.
[9] Hughes CJ, Weimar WH, Sheth PN, Brubaker CE. Biomechanics of wheelchair propulsion as a function of seat position and user-to-chair interface. Arch Phys Med Rehabil 1992;73:263–9.
[10] Gutierrez D, Mulroy SJ, Newsam CJ, Gronley J, Perry J. Effect of fore-aft seat position on shoulder demands during wheelchair propulsion: part 2. An electromyographic analysis. J Spinal Cord Med 2005;28:222–9.
[11] Slowik JS, Requejo PS, Mulroy SJ, Neptune RR. The influence of wheelchair propulsion hand pattern on upper extremity muscle power and stress. J Biomech 2016;49:1554–61. doi:10.1016/j.jbiomech.2016.03.031.
[12] Boninger ML, Souza AL, Cooper RA, Fitzgerald SG, Koontz AM, Fay BT. Propulsion patterns and pushrim biomechanics in manual wheelchair propulsion. Arch Phys Med Rehabil 2002;83:718–23. doi:10.1053/apmr.2002.32455.
[13] de Groot S, Veeger HEJ, Hollander AP, van der Woude LHV. Effect of wheelchair stroke pattern on mechanical efficiency. Am J Phys Med Rehabil 2004;83:640–9. doi:10.1097/01.PHM.0000133437.58810.C6.
[14] Qi L, Wakeling J, Grange S, Ferguson-Pell M. Patterns of shoulder muscle coordination vary between wheelchair propulsion techniques. IEEE Trans Neural Syst Rehabil Eng 2014;22:559–66. doi:10.1109/TNSRE.2013.2266136.
[15] Kwarciak AM, Turner JT, Guo L, Richter WM. The effects of four different stroke patterns on manual wheelchair propulsion and upper limb muscle strain. Disabil Rehabil Assist Technol 2012;7:459–63.
[16] Requejo PS, Furumasu J, Mulroy SJ. Evidence-based strategies for preserving mobility for elderly and aging manual wheelchair users. Top Geriatr Rehabil 2015;31:26–41.
[17] Paralyzed Veterans of America Consortium for Spinal Cord Medicine Preservation of upper limb function following spinal cord injury – a clinical practice guideline for health-care professionals. J Spinal Cord Med 2005;28:434–70.
[18] Leardini A, Chiari L, Della Croce U, Cappozzo A. Human movement analysis using stereophotogrammetry. Part 3. Soft tissue artifact assessment and compensation. Gait Posture 2005;21:212–25.
[19] Šenk M, Chèze L. A new method for motion capture of the scapula using an optoelectronic tracking device: a feasibility study. Comput Methods Biomech Biomed Eng 2010;13:397–401.
[20] van Andel C, van Hutten K, Eversdijk M, Veeger D, Harlaar J. Recording scapular motion using an acromion marker cluster. Gait Posture 2009;29:123–8.
[21] Duprey S, Billuart F, Sah S, Ohl X, Robert T, Skalli W, et al. Three-dimensional rotations of the scapula during arm abduction: evaluation of the acromion marker cluster method in comparison with a model-based approach using biplanar radiograph images. J Appl Biomech 2015;31:396–402.
[22] Lempereur M, Brochard S, Leboeuf F, Rémy-Néris O. Validity and reliability of 3D marker based scapular motion analysis: a systematic review. J Biomech 2014;47:2219–30.
[23] Warner MB, Chappell PH, Stokes MJ. Measuring scapular kinematics during arm lowering using the acromion marker cluster. Hum Mov Sci 2012;31:386–96.
[24] Morrow MMB, Kaufman KR, An K-N. Scapula kinematics and associated impingement risk in manual wheelchair users during propulsion and a weight relief lift. Clin Biomech 2011;26:352–7.
[25] Lu TW, O'Connor JJ. Bone position estimation from skin marker co-ordinates using global optimisation with joint constraints. J Biomech 1999;32:129–34.
[26] Roux E, Bouilland S, Godillon-Maquinghen A-P, Bouttens D. Evaluation of the global optimisation method within the upper limb kinematics analysis. J Biomech 2002;35:1279–83.
[27] Begon M, Bélaise C, Naaim A, Lundberg A, Chèze L. Multibody kinematics optimization with marker projection improves the accuracy of the humerus rotational kinematics. J Biomech 2017;62:117–23.
[28] Michaud B, Duprey S, Begon M. Scapular kinematic reconstruction – segmental optimization, multibody optimization with open-loop or closed-loop chains: which one should be preferred? Int Biomech 2017;4:86–94.
[29] van der Helm FCT. A finite element musculoskeletal model of the shoulder mechanism. J Biomech 1994;27:551555–3569.
[30] Blana D, Hincapie JG, Chadwick EK, Kirsch RF. A musculoskeletal model of the upper extremity for use in the development of neuroprosthetic systems. J Biomech 2008;41:1714–21.
[31] Garner BA, Pandy MG. A kinematic model of the upper limb based on the visible human project (VHP) image dataset. Comput Methods Biomech Biomed Eng 1999;2:107–24.
[32] Naaim A, Moissenet F, Duprey S, Begon M, Chèze L. Effect of various upper limb multibody models on soft tissue artefact correction: a case study. J Biomech 2017;62:102–9.
[33] Bolsterlee B, Veeger HEJ, van der Helm FCT. Modelling clavicular and scapular kinematics: from measurement to simulation. Med Biol Eng Comput 2014;52:283–91.
[34] Holzbaur KRS, Murray WM, Delp SL. A model of the upper extremity for simulating musculoskeletal surgery and analyzing neuromuscular control. Ann Biomed Eng 2005;33:829–40.
[35] Saul KR, Hu X, Goehler CM, Vidt ME, Daly M, Velisar A, et al. Benchmarking of dynamic simulation predictions in two software platforms using an upper limb musculoskeletal model. Comput Methods Biomech Biomed Eng 2015;18:1445–58. doi:10.1080/10255842.2014.916698.
[36] Rankin JW, Richter WM, Neptune RR. Individual muscle contributions to push and recovery subtasks during wheelchair propulsion. J Biomech 2011;44:1246–52. doi:10.1016/j.jbiomech.2011.02.073.
[37] Morrow MM, Rankin JW, Neptune RR, Kaufman KR. A comparison of static and dynamic optimization muscle force predictions during wheelchair propulsion. J Biomech 2014;47:3459–65. doi:10.1016/j.jbiomech.2014.09.013.
[38] Slowik JS, McNitt-Gray JL, Requejo PS, Mulroy SJ, Neptune RR. Compensatory strategies during manual wheelchair propulsion in response to weakness in individual muscle groups: a simulation study. Clin Biomech 2016;33:34–41. doi:10.1016/j.clinbiomech.2016.02.003.
[39] de Groot JH, Brand R. A three-dimensional regression model of the shoulder rhythm. Clin Biomech (Bristol, Avon) 2001;16:735–43.
[40] Pronk GM. The shoulder girdle: analysed and modelled kinematically. The Netherlands: Delft University of Technology; 1991.
[41] Van der Helm FCT, Veeger HEJ, Pronk GM, Van der Woude LHV, Rozendal RH. Geometry parameters for musculoskeletal modelling of the shoulder system. J Biomech 1992;25:129–44.
[42] Seth A, Sherman M, Eastman P, Delp S. Minimal formulation of joint motion for biomechanisms. Nonlinear Dyn 2010;62:291–303.
[43] Seth A, Matias R, Veloso AP, Delp SL, Harlaar J, Sciascia A. A biomechanical model of the scapulothoracic joint to accurately capture scapular kinematics during shoulder movements. PLoS One 2016;11:e0141028.
[44] Dabonneville M, Vaslin P, Kauffmann P, de Saint Rémy N, Couétard Y, Cid M. A self-contained wireless wheelchair ergometer designed for biomechanical measures in real life conditions. Technol Disabil 2005;17:63–76.
[45] Hybois S, Siegel A, Bascou J, Eydieux N, Vaslin P, Pillet H, et al. Shoulder kinetics during start-up and propulsion with a manual wheelchair within the initial phase of uninstructed training. Disabil Rehabil Assist Technol 2018;13:40–6.
[46] Sauret C, Faye V, Bascou J, Pillet H, Lavaste F. Handrim mechanical power during wheelchair propulsion on level and cross-slope surfaces: a preliminary study. Comput Methods Biomech Biomed Eng 2013;16:124–5. doi:10.1080/10255842.2013.815882.
[47] Söderkvist I, Wedin PA. Determining the movements of the skeleton using well-configured markers. J Biomech 1993;26:1473–7.
[48] Delp SL, Anderson FC, Arnold AS, Loan P, Habib A, John CT, et al. OpenSim: open-source software to create and analyze dynamic simulations of movement. IEEE Trans Biomed Eng 2007;54:1940–50.
[49] Cooper RA, Boninger ML, Shimada SD, Lawrence BM. Glenohumeral joint kinematics and kinetics for three coordinate system representations during wheelchair propulsion. Am J Phys Med Rehabil 1999;78:435–46.
[50] Desroches G, Aissaoui R, Bourbonnais D. Effect of system tilt and seat-to-backrest angles on load sustained by shoulder during wheelchair propulsion. J Rehabil Res Dev 2006;43:871.
[51] Wu G, van der Helm FC, Veeger HEJ, Makhsous M, Van Roy P, Anglin C. l. ISB recommendation on definitions of joint coordinate systems of various joints for the reporting of human joint motion—Part II: shoulder, elbow, wrist and hand. J Biomech 2005;38:981–92.
[52] Blache Y, Begon M. Influence of shoulder kinematic estimate on joint and muscle mechanics predicted by musculoskeletal model. IEEE Trans Biomed Eng 2017;65(4):715–22.
[53] Van Drongelen S, Van der Woude LH, Janssen TW, Angenot EL, Chadwick EK, Veeger DH. Mechanical load on the upper extremity during wheelchair activities. Arch Phys Med Rehabil 2005;86:1214–20. doi:10.1016/j.apmr.2004.09.023.

[54] Vegter RJK, Hartog J, de Groot S, Lamoth CJ, Bekker MJ, van der Scheer JW, et al. Early motor learning changes in upper-limb dynamics and shoulder complex loading during handrim wheelchair propulsion. J Neuroeng Rehabil 2015;12:26. doi:10.1186/s12984-015-0017-5.
[55] Morrow MMB, Hurd WJ, Kaufman KR, An K-N. Upper-limb joint kinetics expression during wheelchair propulsion. J Rehabil Res Dev 2009;46:939. doi:10.1682/JRRD.2008.12.0165.
[56] Collinger JL, Boninger ML, Koontz AM, Price R, Sisto SA, Tolerico ML, et al. Shoulder biomechanics during the push phase of wheelchair propulsion: a multisite study of persons with paraplegia. Arch Phys Med Rehabil 2008;89:667–76.
[57] Mercer JL, Boninger M, Koontz A, Ren D, Dyson-Hudson T, Cooper R. Shoulder joint kinetics and pathology in manual wheelchair users. Clin Biomech (Bristol, Avon) 2006;21:781–9. doi:10.1016/j.clinbiomech.2006.04.010.
[58] Van Drongelen S, Van der Woude LH, Janssen TW, Angenot EL, Chadwick EK, Veeger DH. Mechanical load on the upper extremity during wheelchair activities. Arch Phys Med Rehabil 2005;86:1214–20.
[59] Sabick MB, Kotajarvi BR, An K-N. A new method to quantify demand on the upper extremity during manual wheelchair propulsion. Arch Phys Med Rehabil 2004;85:1151–9.
[60] Veeger HEJ, Rozendaal LA, van der Helm FCT. Load on the shoulder in low intensity wheelchair propulsion. Clin Biomech 2002;17:211–18. doi:10.1016/S0268-0033(02)00008-6.
[61] Koontz AM, Cooper RA, Boninger ML, Souza AL, Fay BT. Shoulder kinematics and kinetics during two speeds of wheelchair propulsion. J Rehabil Res Dev 2002;39:635–49.
[62] O'Reilly OM, Sena MP, Feeley BT, Lotz JC. On representations for joint moments using a joint coordinate system. J Biomech Eng 2013;135:114504. doi:10.1115/1.4025327.
[63] Desroches G. Expression of joint moment in the joint coordinate system. J Biomech Eng 2010;132:114503. doi:10.1115/1.4002537.
[64] Eydieux N, Hybois S, Siegel A, Bascou J, Vaslin P, Pillet H, et al. Changes in wheelchair biomechanics within the first 120 minutes of practice: spatiotemporal parameters, handrim forces, motor force, rolling resistance and fore-aft stability. Disabil Rehabil Assist Technol 2019;20:1–9. doi:10.1080/17483107.2019.1571117.
[65] Karduna AR, McClure PW, Michener LA, Sennett B. Dynamic measurements of three-dimensional scapular kinematics: a validation study. J Biomech Eng 2001;123:184–90.